3 1176 00168 0793

NASA TM-81704

NASA Technical Memorandum 81704

NASA-TM-81704 19810014655

Traction Drive for Cryogenic Boost Pump

FOR REFERENCE

NOT TO BE TAKEN FROM THIS ROOM

Scott Meyer and R. E. Connelly
Lewis Research Center
Cleveland, Ohio

March 1981

NASA

SUMMARY

Two versions of a Nasvytis Multiroller Traction Drive were tested in liquid oxygen for possible application as cryogenic boost pump speed reduction drives for advanced hydrogen-oxygen rocket engines. The roller drive, with a 10.8:1 reduction ratio, was successfully run at up to 70 000 rpm input speed and up to 14.9 kW (20 hp) input power level. Three drive assemblies were tested for a total of about three hours of which approximately one hour was at nominal full speed and full power conditions. Peak efficiency of 60 percent was determined. There was no evidence of slippage between rollers for any of the conditions tested. The ball drive, a version using balls instead of one row of rollers, and having a 3.25:1 reduction ratio, failed to perform satisfactorily.

INTRODUCTION

Advanced high chamber pressure hydrogen-oxygen rocket engines require efficient, high-speed, high-pressure propellant turbopumps. These high-speed pumps require a moderately high inlet pressure for operation. Low-speed boost pumps are generally used to supply the required inlet pressure to the high-speed main turbopumps to keep the propellant tank pressure and weight to a minimum. The boost pumps may be driven by gas or hydraulic turbines, but these require complex valving and speed control systems. Another option is to drive the boost pumps through a mechanical speed reduction drive directly coupled to the main turbopumps. This speed reduction drive must operate completely submerged in the cryogenic fluid which provides cooling, but no lubrication. Gear reduction drives have been successfully operated in cryogenic fluids, but are questionable for the expected 10-hour life requirement at the very high turbopump speeds of future rocket engines (refs. 1 and 2). The Nasvytis Multiroller Traction Drive (ref. 3) has the potential to attain the required life. The traction drive uses smooth rollers to transmit power and thus the life problems associated with sliding contact in gear teeth are eliminated. The planetary traction drive has proved to be reliable and efficient in commercial applications (ref. 4), but there has been no attempt to adapt the drive to cryogenic applications.

The objective of the work described was to evaluate the potential of the traction drives for the above cryogenic application. Tests were run on a Nasvytis Multiroller Drive having a 10.8:1 ratio, and a variation of the Nasvytis drive, the ball drive, with a 3.25:1 ratio. Tests were run in liquid oxygen, including steady state and transient tests, at shaft speeds up to 70 000 rpm and input powers up to 14.9 kW (20 hp).

N81-23188#

APPARATUS

Test Drives

Two types of traction drives were tested in this study. The drives were designed for a speed and power range required for driving liquid oxygen and liquid hydrogen boost pumps required for an 88 964 N (20 000 lbf) thrust rocket engine. The design data for these drives are shown in table I.

The Nasvytis Multiroller Drive, designed for the LOX boost pump at a speed ratio of 10.8:1, is shown in figures 1, 2, and 3. The roller drive consists of two rows of five planet rollers contained between the concentric sun and ring rollers. The second row of rollers transmits the reaction torque to the housing through ball bearings mounted on the roller shafts. The sun roller, figure 4, is split to provide a means of providing roller contact load proportional to the input torque. The first and second row rollers are shown in figure 5.

The ball drive, which is a modification of the roller drive, is shown in figures 6 and 7. It was designed for the hydrogen boost pump at a speed ratio of 3.25:1. The ball drive has two rows of eight planets contained between the concentric sun and ring rollers. The first row of planets is made up of sixteen balls. As in the roller drive, the sun roller is split to provide a loading mechanism for the drive. The second row planets and the first row balls are shown in Figure 8.

The sun rollers and the planet rollers were fabricated from AISI 440C stainless steel that was through hardened to a Rockwell-C hardness of 58 to 60. The ring roller consisted of a hardened AISI 440C liner interference fitted in an Inconel 718 output ring. All roller running surfaces were ground to surface finishes from 0.2 to 0.4 μm (8 to 16 μin.) rms. The remaining drive components were fabricated from Inconel 718.

The roller loading mechanism for the drives are similar. The loading mechanism adjusts the normal contact load between the rollers in proportion to the transmitted torque, effectively maintaining a constant traction coefficient. This torque-responsive loading mechanism insured that sufficient normal load was applied under all conditions to prevent slip, without needlessly overloading the contacts at light loads. The mechanism was designed to operate above some preselected, mechanically adjusted minimum preload. The roller drive high-speed or input shaft with the split sun roller and loading mechanism is shown in figure 4. The surfaces of the sun roller halves which contact the first row planet rollers are tapered (3° in this case) so that as the space between them decreases, the first row planets are forced radially outward loading the drive. The axially inward force of the sun halves is provided by tapered lands milled into the back faces of the sun halves and oppositely milled lands in the faces of the drive cams, figure 9. The drive cams are keyed to the high-speed shaft and lightly spring loaded axially so that there is contact between the drive rollers under zero torque condition.

As input torque is applied, equal and opposite axial loading is applied to the sun halves from the drive cams through the cam loading balls by the action of the milled tapered lands. The roller contact is proportional to the input torque with the proportionality constant determined by the selection of the angle of the tapered lands and the taper angle of the sun rollers.

Test Rig

The multiroller drives were tested in a fixture as shown in figure 10. A test facility schematic is shown in figure 11. The test fixture consisted of three major elements; the housing, the turbine and the brake.

The drives were mounted in a sealed housing that contained the coolant and directed it to the desired areas of the drive. The coolant flow divided after entering the housing, with approximately 20 percent flowing through the high speed shaft bearings and the remainder cooling the drive rollers. Separate coolant drains were provided and inlet and outlet coolant temperatures and pressures were measured. The coolant pressure was maintained at 4.5×10^5 N/m^2 (65 psi) to suppress cryogenic coolant boiling within the drive.

A radial flow turbine driven by nitrogen gas provided input power to the drives. Speed control was accomplished with a control valve in the turbine gas supply line. An eddy current proximity probe monitored the passage of the turbine blades and provided a shaft speed signal. A closed loop controller maintained shaft speed constant.

The output power was absorbed with a radial flow turbine driven by nitrogen gas and operating in reverse. The power absorbed by the brake and thus the power transmitted through the drive was varied by means of a control valve in the brake turbine gas supply line. The passage of the brake turbine blades was monitored by a proximity probe to indicate brake speed.

Simple shaft seals were provided to isolate the liquid oxygen coolant from the nitrogen drive gas for the turbine and the brake. The seals consisted of a nitrogen purged cavity between the oxygen and the turbine drive gas. Pressure in this cavity was maintained slightly higher than the coolant pressure.

Turbine and Brake Calibration Rig

The performance of the turbine and the brake was characterized using a separate calibration fixture. In this fixture the turbine and brake were mounted on separate shafts, each supported by ball bearings. These two shafts were then connected by a splined guill shaft containing a calibrated torque transducer. The torque signal was brought out through high-speed slip rings to the signal conditioning equipment. Data

were gathered by operating the calibration rig at a constant speed and varying the applied torque. Turbine inlet pressure, outlet pressure, brake inlet pressure and outlet pressure, shaft speed and torque were measured at shaft speeds up to 40 000 rpm. Inadequate bearing lubrication and cooling prevented operation at higher shaft speeds. Operation of the rig without the brake wheel attached allowed the measurement of the test fixture bearing losses. The data gathered related the turbine torque as a function of turbine inlet pressure and also the brake torque as a function of brake inlet pressure. This data allowed the calculation of input power and output power during the testing of the multiroller drives. Although data were gathered at up to 40 000 rpm the results were extrapolated to 70 000 rpm. The error in this extrapolation is estimated to be 5 percent or less.

PROCEDURE

Prior to each test, the drives were completely disassembled and the parts were cleaned in an ultrasonic cleaner to assure compatibility with liquid oxygen. After reassembly, the drives were installed in the test fixture and the fixture was mounted in the facility.

Liquid oxygen was slowly flowed through the drive for approximately one-half hour to pre-cool all parts to liquid oxygen temperature. Once the desired temperature was reached, the turbine was driven up to the desired speed following a linear speed ramp. The final speed and the ramp rate were adjustable. Ramp rates of 30 minutes to 5 seconds to full speed were run. Once at speed, the brake turbine flow was applied to load up the drive. Data was recorded at several power levels before the brake was shut off and the drive decelerated slowly to zero speed.

For any turbine inlet pressure and turbine speed the turbine torque, and thus the drive input torque, could be found from the turbine calibration data. The product of turbine torque and turbine speed yielded the drive input power. Similar calculations, based upon the brake inlet pressure and brake speed, yielded the output power of the drives. The ratio of the drive output power to the input power is the drive efficiency.

RESULTS AND DISCUSSION

Check-Out Tests

The roller and ball drives were tested in oil mist, liquid nitrogen and liquid oxygen. The oil mist and liquid nitrogen tests were run to check out the drives for proper assembly and mechanical operation in a less hazardous and more convenient fluid than liquid oxygen. No significant data were obtained during the checkout tests. Test speeds of 70 000 rpm were attained, but all the testing was done at essentially no load.

Roller Drive Tests

The roller drive tests in liquid oxygen accumulated a total test time of about three hours, of which about one hour was at the design speed of 70 000 rpm. Data were obtained at speeds between 20 000 and 70 000 rpm, while input power was varied from 1.5 to 14.9 kW (2 to 20 hp). The drive efficiency ranged from 10 percent to 60 percent. Three sets of roller drive hardware were used and each assembly was tested to failure. In each of the test series, data were obtained by slowly ramping the drive speed up to design speed and varying the drive load from minimum to design torque at selected values of drive speed. In the last test series, the last two tests were cyclic tests in which the drive speed was accelerated to design speed in 10 seconds and in 5 seconds. A summary of the data is presented in table II.

The first set of roller drive hardware survived four tests for 72 minutes total duration. The failure was attributed to the failure of the AISI 440C liner to remain seated in the low-speed shaft housing, figure 12. The liner was a shrink fit for this test. The liner was pinned in place in subsequent assemblies. The sun and planet rollers are shown in figures 13 and 5. The first and second row planets shown in figure 5 were in good condition after the test. The sun rollers in figure 13 show the effects of possible inadequate local cooling although no sign of excessive heating was detected in the coolant temperature rise data.

The second set of hardware shown in figures 14, 15, 16, and 17 failed after 42 minutes in three tests. Post test inspection revealed evidence of a fire on the high-speed shaft and failed high-speed shaft bearing (fig. 14). No conclusion was reached whether the fire or bearing failure occurred first. The first and second row rollers (figs. 15 and 16) were in fair condition while the sun rollers (fig. 17) showed considerable distress.

The third set of hardware accumulated 43 minutes in six tests before failing. The last two tests of this series were cyclic tests in which the drive was rapidly accelerated to design speed. Seventeen cycles were run at a ramp speed of 7000 rpm per second and 15 cycles at 14 000 rpm per second. At the end of each speed ramp, the input torque was varied from minimum to design value. At the end of the fifteenth cycle and at an input torque of 2.26 N-m (20 in-lbf), the drive failed. The output torque at failure was 12.43 N-M (110 in-lbf) for a drive efficiency of 50.9 percent. The sun, first row planets, second row planets and ring roller are shown in figures 18, 19, 20, and 21. The sun roller (fig. 18) indicates high loading or insufficient cooling as in the previous tests. The planets (figs. 19 and 20) are shown to be in fair condition. The actual cause of failure appears to be due to failure of the planet bearings. The inner races of the failed bearings are shown still mounted on the planet shafts. The outer races are shown in the housing in figure 22.

In all of the roller drive tests the ratio between the input and output speeds was constant. Within the limits of the speed measurement accuracy no slippage could be detected. The results of the roller drive tests are shown in figure 23. The output power against the input power is shown with input shaft speed and percent design input torque as parameters. The roller drive power loss is significantly more dependent upon speed than upon torque. This result is in agreement with the results of the tests reported in refence 5. The constant speed lines of 50 000 rpm and above have the same slope as the 100 percent efficiency or zero loss line; therefore, increasing input torque at constant speeds results in a constant power loss and an increase in drive efficiency. At lower speeds, the power loss is dependent upon both torque input and speed.

Ball Drive Tests

The ball drive tests in liquid oxygen were not successful. In most tests, the drive locked up and failed to rotate. Post test inspections gave no indication of the cause of its failure to operate. After several reassemblies and repeated failures, the testing of the ball drive was discontinued. It is possible that the drive is inherently unstable because of failure to maintain parallelism between four of the second row planet axes and the ring roller axis. Four of the eight second row planets were supported and kept in alignment with ball bearings while four of the planet rollers were permitted to "float" between the first row balls and the ring roller (fig. 8).

CONCLUDING REMARKS

The roller drive tests in liquid oxygen indicate that the Nasvytis drive can be developed into a useful transmission for cryogenic applications. None of the three failures which occurred could be attributed to failure of the rollers. The sun roller did show distress in all three tests, but this may be due to excessive roller loading. Because no slippage was observed, it may be possible to reduce the roller loading from that used in these tests. In addition, it may be possible to improve the cooling of the sun rollers and, consequently, improve their life.

The efficiencies obtained were lower than those obtained in tests described in reference 5 probably because of windage losses due to operation submerged in liquid oxygen. The tests in reference 5 were run using oil as a lubricant with the housing kept relatively dry with the use of a scavenger pump. In addition, the rollers sustained mechanical damage during the testing resulting in additional losses.

A basic problem with the drives is that without perfect parallelism between the centerlines of the second row rollers and the ring roller, an axial force is generated between the second row rollers and the ring. This misalignment is what caused the

ring roller insert to be forced from its proper location in the ring casing in the first test series. This form of instability may be relieved by application of the stability criteria as described in reference 6. The failure of the ball drive was probably caused by the skewing of the floating second row planet rollers which were not maintained parallel to the ring roller. A design change in which all of second row rollers were bearing supported would relieve most of this problem.

SUMMARY OF RESULTS

A Nasvytis Multiroller Traction Drive with a 10.8:1 ratio and a modification of the Nasvytis Drive, the Ball Drive, with a 3.25:1 ratio were tested in liquid oxygen. Input speeds to 70 000 rpm and input power levels to 14.9 kW (20 hp) were run with the following results:

1. Peak efficiency of 60 percent was determined.
2. Three drives were tested for a total of 3 hours, of which 1 hour was at full speed and full power.
3. The drive power losses at speeds above 40 000 rpm were significantly affected by speed and insensitive to variations in input torque.
4. There was no evidence of slippage between rollers detected within the limits of the speed measuring accuracy.
5. The Ball Drive failed to rotate or "locked up" after a few revolutions in every test.

REFERENCES

1. Zachary, A. T.: Advanced Space Engine Preliminary Design. (R-9269, Rocketdyne; NASA Contract NAS3-16751.) NASA CR 121236, 1973.
2. Cuffe, J. P. B.; and Bradie, R. E.: Advanced Space Engine Preliminary Design. (PWA-FR-5654, Pratt and Whitney Aircraft; NASA Contract NAS3-16750.) NASA CR 121237, 1973.
3. Nasvytis, Algirdas L.: Multiroller Planetary Friction Drives. SAE Paper 660763, Oct. 1966.
4. Carson, Robert W.: Traction Drives Update. Power Transm. Des., vol. 19, no. 11, Nov. 1977, pp. 37-42.
5. Loewenthal, Stuart H.; Anderson, Neil E.; and Nasvytis, Algirdas L.: Performance of a Nasvytis Multiroller Traction Drive. NASA TP-1378, 1978.
6. Savage, Michael; and Loewenthal, Stuart H.: Kinematic Stability of Roller Pairs in Free-Rolling Contact. NASA TN D-8146, 1976.

TABLE I. - DESIGN DATA

	Roller drive	Ball drive
1. Input speed, rpm	70 000	95 000
2. Output speed, rpm	6475	29 238
3. Reduction ratio	10.8:1	3.25:1
4. Power, kW (hp)	11.2 (15)	22.4 (30)
5. Torque, Nm (in-lbf)	1.52 (13.5)	2.25 (19.9)
6. O.D. low speed shaft, cm (in)	8.89 (3.5)	8.89 (3.5)
7. Overall length, cm (in)	22.85 (9.0)	22.85 (9.0)
8. Drive weight, kg (lb)	4.1 (9.0)	4.3 (9.5)
9. Ring roller dia., cm (in)	6.85 (2.697)	7.64 (3.007)
10. Sun roller dia., cm (in)	1.23 (0.500)	2.14 (0.841)
11. First row roller dia., cm (in)	1.69 (0.666) 0.84 (0.332)	1.19 (0.469)
12. Second row roller dia., cm (in)	2.09 (0.824)	2.01 (0.790) 1.77 (0.700)
13. Assumed coefficient of friction	0.06	0.06
14. Roller contact stress, N/m^2 (lbf/in^2)	1.25×10^9 (181 600)	5.45×10^8 (79 000)
15. Planet bearing DN, RPM × Bore (mm)	134 000	723 000
16. Roller material	440C	440C

TABLE II.- SUMMARY OF RESULTS, ROLLER DRIVE LOX TESTS

Drive assembly	Input speed, rpm	Input power		Output power		Efficiency	Duration, sec	Rate, rpm/sec	Reason for test termination
		kW	hp	kW	hp				
1	10 011	0.77	1.03	0.47	0.63	0.61	(a)	33.3	
	21 118	3.21	4.30	1.92	2.57	.60			
	32 623	4.55	6.10	2.45	3.28	.54			
	42 086	7.38	9.90	4.16	5.58	.56			
	52 196	9.92	13.3	6.03	8.09	.61			
	60 414	11.26	15.1	6.23	8.35	.55			
	70 873	12.83	17.2	5.18	6.94	.40	1738	77.7	Sun rollers worn
2	41 720	6.49	8.70	4.03	5.40	.62	1354	38.9	
	70 000	(b)					1600	77.7	
	40 000	(b)					161	248.4	Drive siezed
3	70 000	(b)					924	116.7	
	69 678	11.63	15.6	4.40	5.90	.38	735	233.3	
	49 296	4.37	5.86	1.33	1.79	.30	392	166.7	
	69 533	6.50	8.72	.30	.40	.05	182	7000 17 cycles	
	69 383	15.59	20.9	8.43	11.3	.54	392	14 000 15 cycles	Drive siezed

[a] Continuous ramp to 60 000 rpm for 1927 sec total duration.

[b] Data lost.

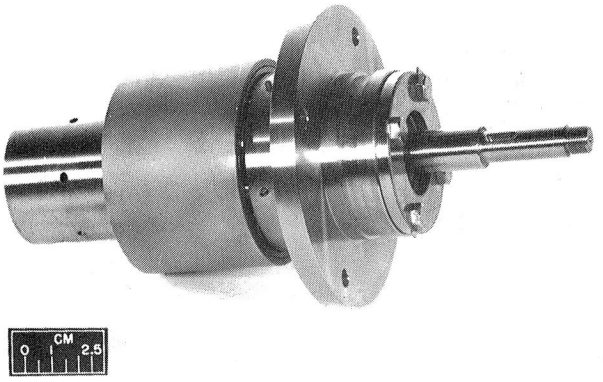

Figure 1. - Roller drive. C-76-4809

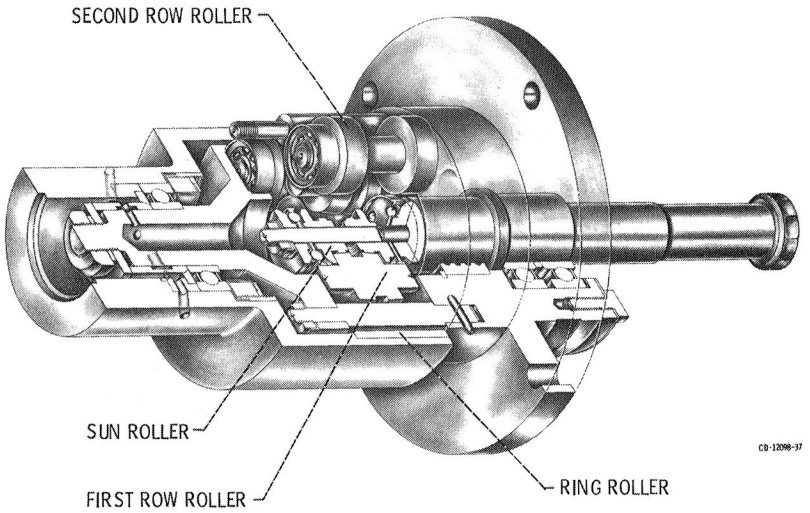

Figure 2. - Roller drive, cutaway view.

CD-12098-37

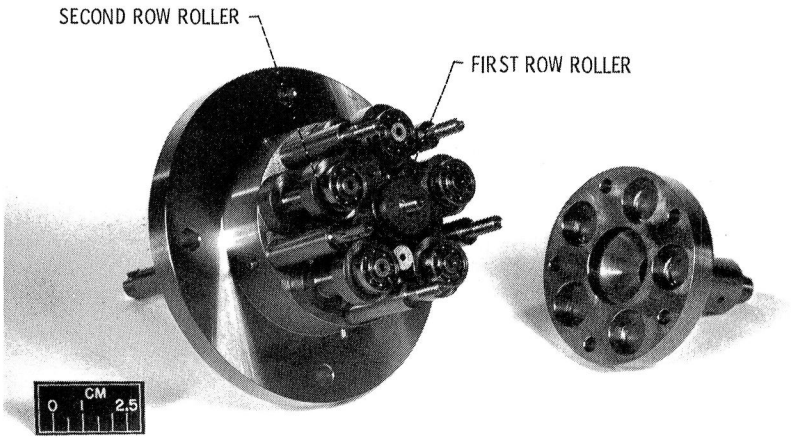

Figure 3. - Roller drive, partially disassembled.

C-76-4801

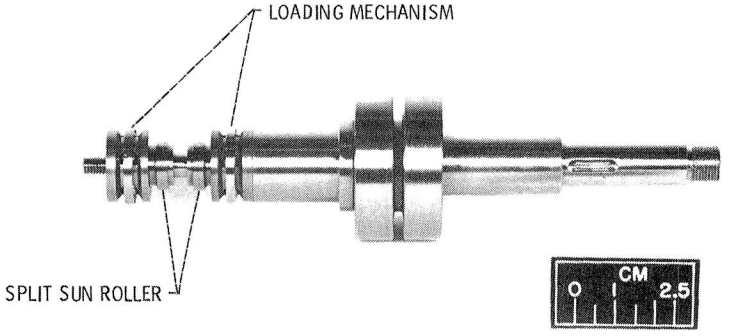

Figure 4. - High speed shaft assembly.

C-76-4803

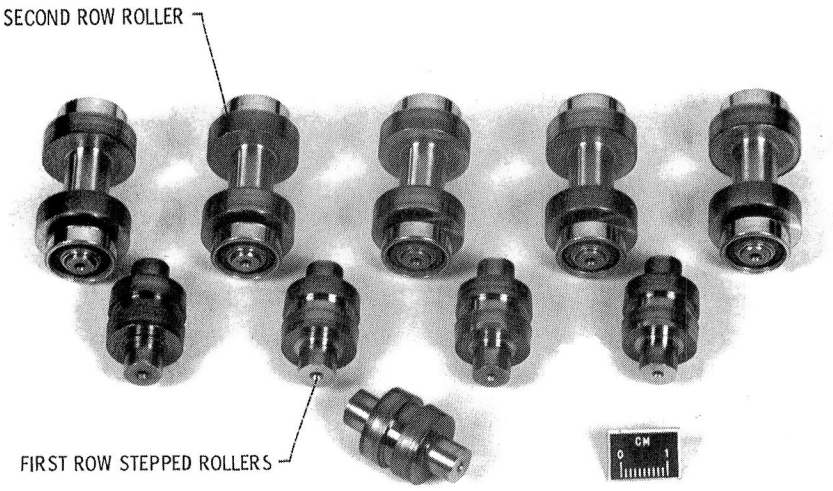

Figure 5. - Roller drive, first & second row rollers.

C-79-1329

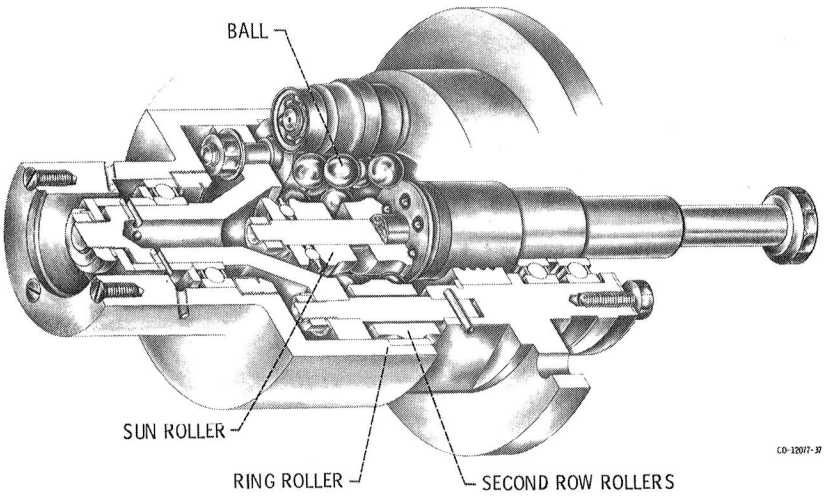

Figure 6. - Ball drive, cutaway view.

CD-12077-37

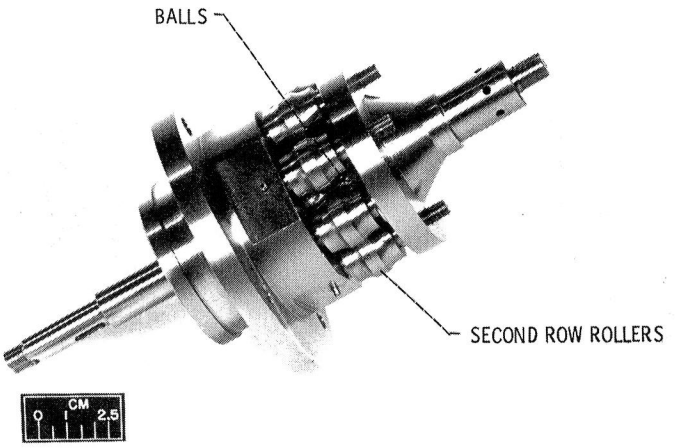

Figure 7. - Ball drive, partially disassembled.

C-76-4808

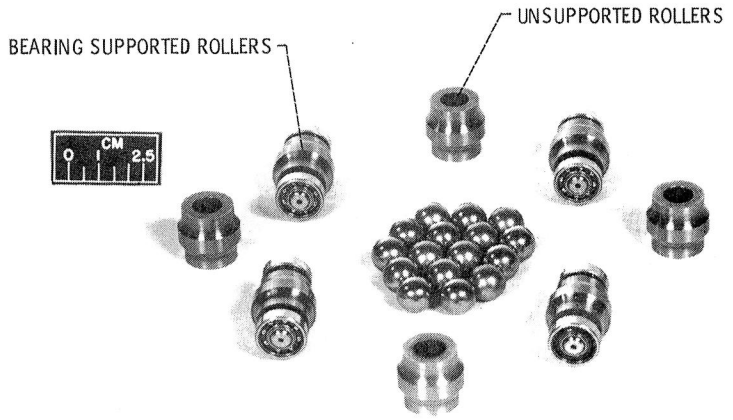

Figure 8. - Ball drive, second row rollers and balls.

C-76-4805

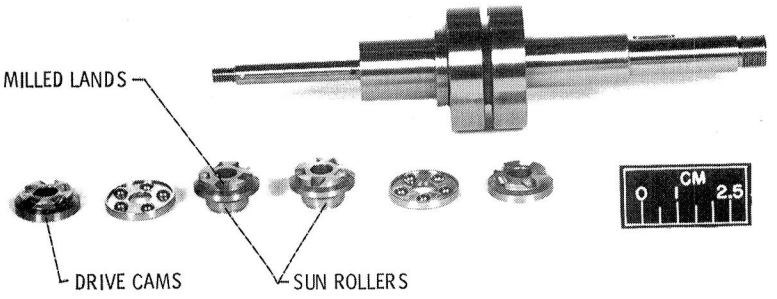

Figure 9. - Roller drive, loading mechanism.

C-76-4804

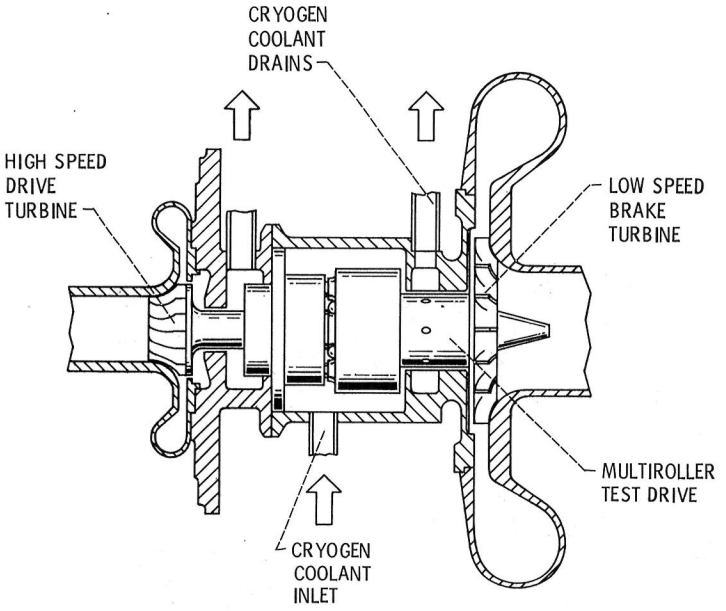

Figure 10. - Test fixture.

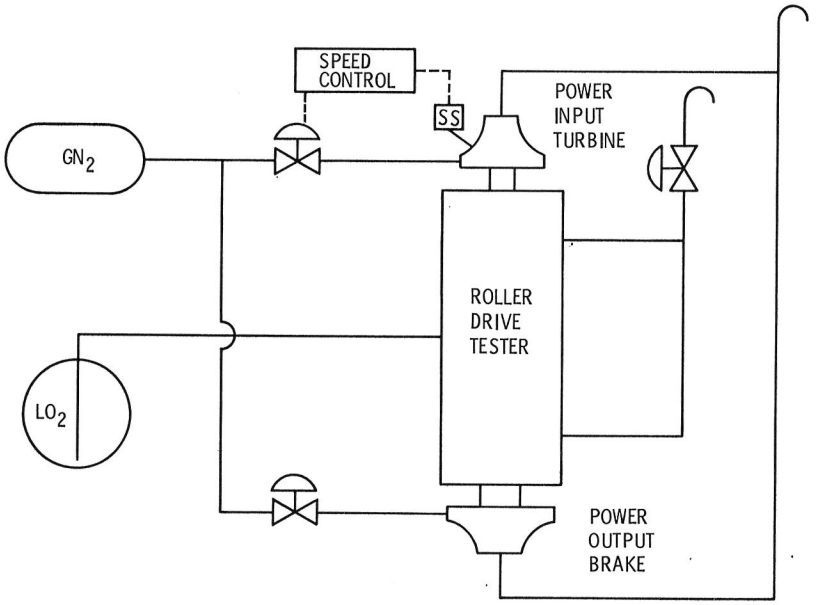

Figure 11. - Facility schematic.

C-76-4801

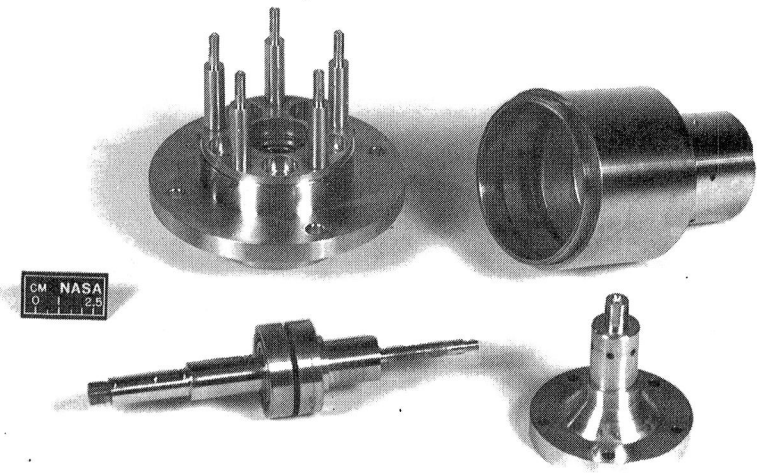

Figure 12. - Roller drive No. 1, after testing.

C-79-1331

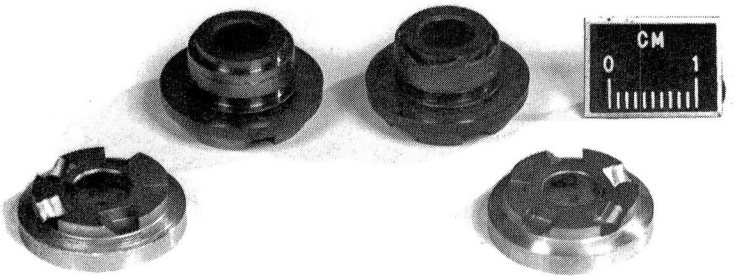

Figure 13. - Roller drive No. 1, sun rollers after testing.

C-79-1330

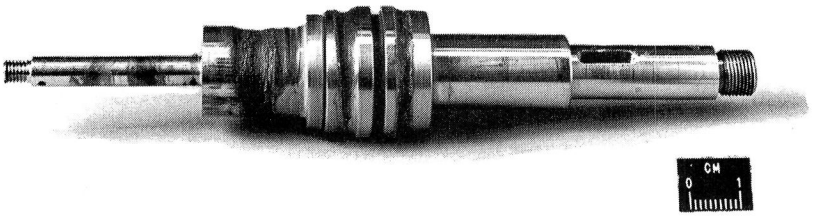

Figure 14. - Roller drive No. 2, shaft after testing.

C-80-2573

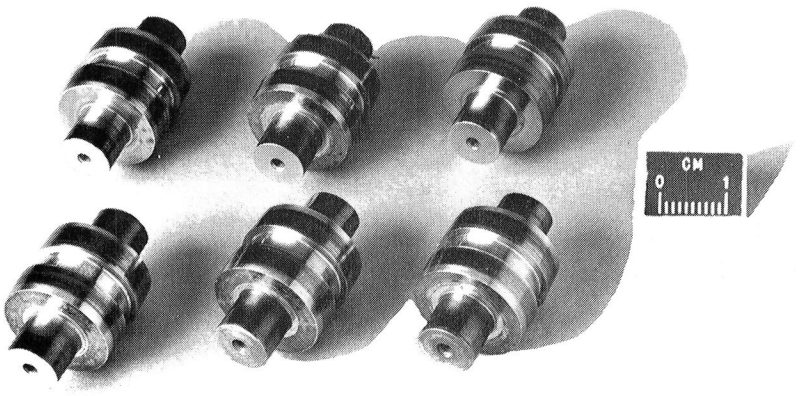

Figure 15. - Roller drive No. 2, first row rollers after testing.

C-80-2574

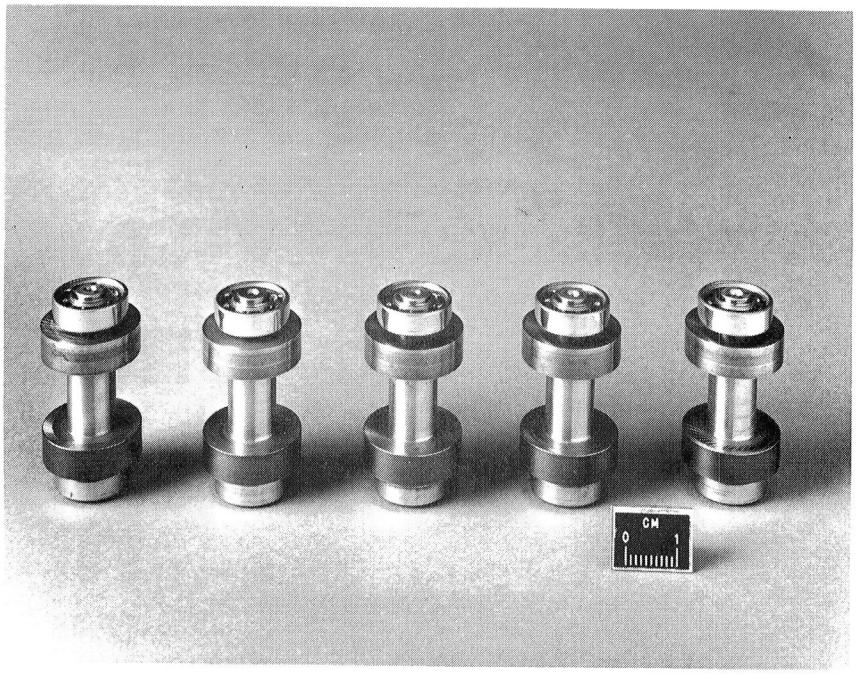

Figure 16. - Roller drive No. 2, second row rollers after testing.

C-80-2572

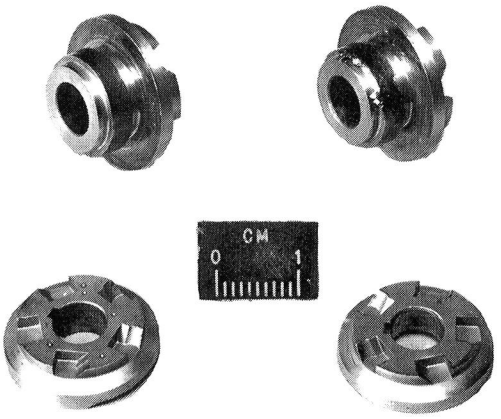

Figure 17. - Roller drive No. 2, sun rollers after testing.

C-80-2997

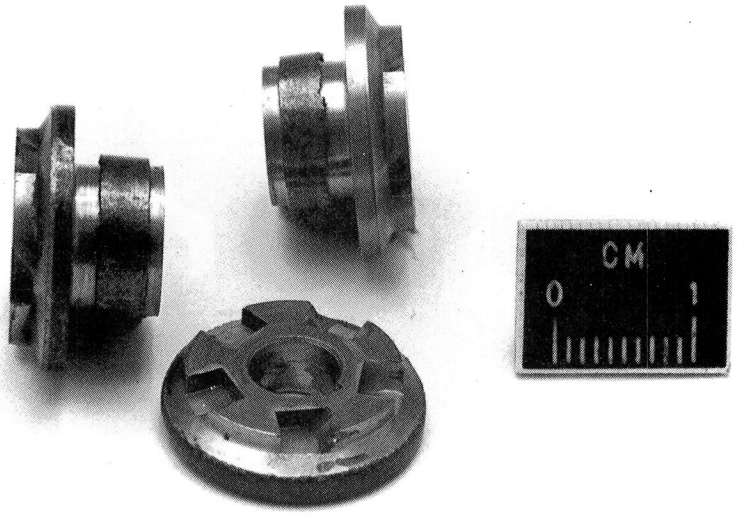

Figure 18. - Roller drive No. 3, sun rollers after testing.

C-80-0790

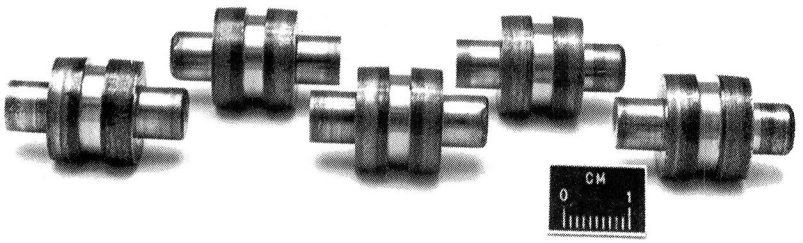

Figure 19. - Roller drive No. 3, first row rollers after testing.

C-80-0791

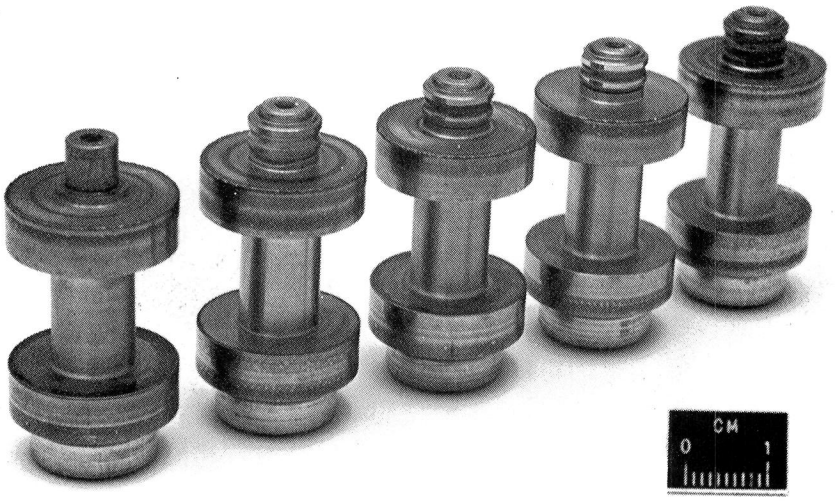

Figure 20. - Roller drive No. 3, second row rollers after testing.

C-80-0788

Figure 21. - Roller drive No. 3, ring roller after testing.
C-80-0792

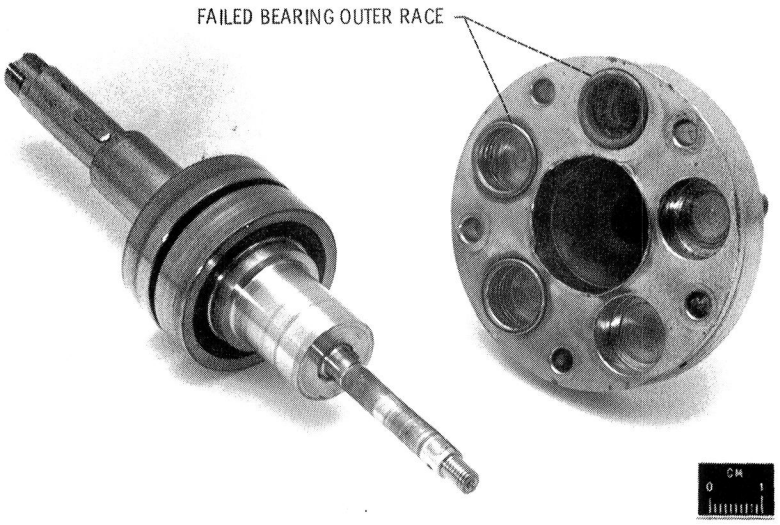

Figure 22. - Roller drive No. 3, shaft and cap, showing second row roller bearing failure.
C-80-0789

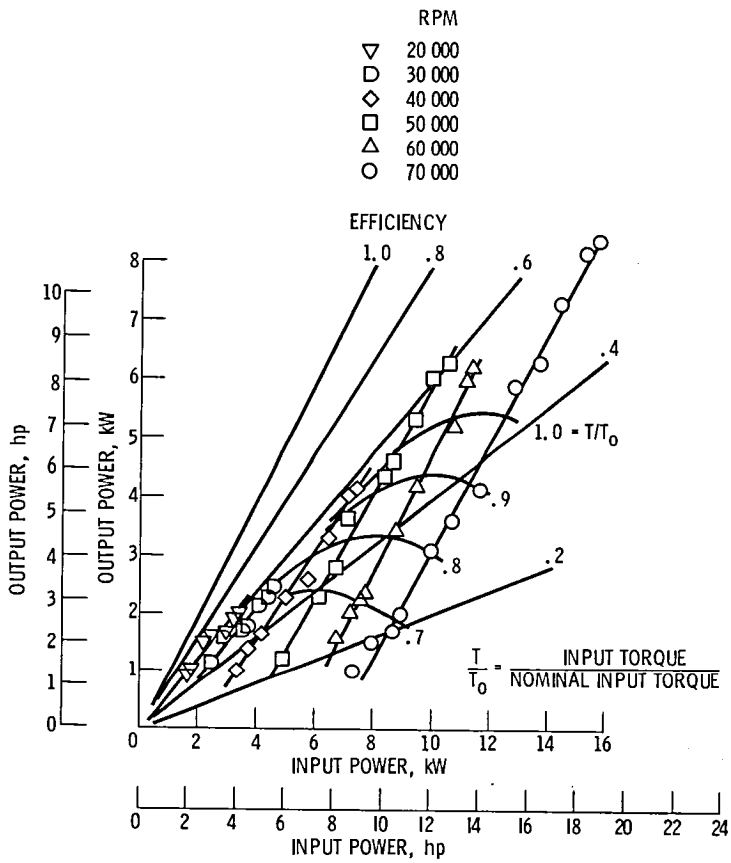

Figure 23. - Rollerdrive performance in liquid oxygen.

1. Report No.	2. Government Accession No.	3. Recipient's Catalog No.
NASA TM-81704		

4. Title and Subtitle	5. Report Date
TRACTION DRIVE FOR CRYOGENIC BOOST PUMP	March 1981
	6. Performing Organization Code: 506-52-12
7. Author(s): Scott Meyer and R. E. Connelly	8. Performing Organization Report No.: E-730
	10. Work Unit No.
9. Performing Organization Name and Address: National Aeronautics and Space Administration, Lewis Research Center, Cleveland, Ohio 44135	11. Contract or Grant No.
	13. Type of Report and Period Covered: Technical Memorandum
12. Sponsoring Agency Name and Address: National Aeronautics and Space Administration, Washington, D.C. 20546	14. Sponsoring Agency Code

15. Supplementary Notes

16. Abstract

Two versions of a Nasvytis Multiroller Traction Drive were tested for possible application as cryogenic boost pump speed reduction drives for advanced hydrogen-oxygen rocket engines. Results are presented for a 10.8:1 speed ratio unit and a modified unit, the Ball Roller Drive, with a 3.25:1 speed ratio. The tests were run in liquid oxygen, including steady state and transient operation at input speeds up to 70 000 rpm and input powers up to 14.9 kW (20 hp). Maximum power transmission efficiency was 60 percent, with no evidence of slippage.

17. Key Words (Suggested by Author(s))	18. Distribution Statement
Boost pump drive; Traction drive; Liquid oxygen-liquid hydrogen turbopump drive; Rocket engine turbopump; Cryogenic turbopump drive; Speed reduction drive	Unclassified - unlimited STAR Category 20

19. Security Classif. (of this report)	20. Security Classif. (of this page)	21. No. of Pages	22. Price*
Unclassified	Unclassified		

* For sale by the National Technical Information Service, Springfield, Virginia 22161

National Aeronautics and
Space Administration

Washington, D.C.
20546

Official Business
Penalty for Private Use, $300

SPECIAL FOURTH CLASS MAIL
BOOK

Postage and Fees Paid
National Aeronautics and
Space Administration
NASA-451

NASA

POSTMASTER: If Undeliverable (Section 158
Postal Manual) Do Not Return